

Degradation of the Mitotic Cyclin Clb3 Is not Required for Mitotic Exit but Is Necessary for G₁ Cyclin Control of the Succeeding Cell Cycle

Kresti Pecani and Frederick R. Cross¹

Laboratory of Cell Cycle Genetics, The Rockefeller University, New York, New York 10065

ABSTRACT B-type cyclins promote mitotic entry and inhibit mitotic exit. In *Saccharomyces cerevisiae*, four B-type cyclins, Clb1–4, carry out essential mitotic roles, with substantial but incomplete overlap of function among them. Previous work in many organisms has indicated that B-type cyclin-dependent inhibition of mitotic exit imposes a requirement for mitotic destruction of B-type cyclins. For instance, precise genomic removal of the Clb2 destruction box (D box) prevents mitotic proteolysis of Clb2, and blocks mitotic exit. Here, we show that, despite significant functional overlap between Clb2 and Clb3, D-box-dependent Clb3 proteolysis is completely dispensable for mitotic exit. Removal of the Clb3 D box results in abundant Clb3 protein and associated kinase throughout the cell cycle, but mitotic exit occurs with close to normal timing. Clb3 degradation is required for pre-Start G₁ control in the succeeding cell cycle. Deleting the *CLB3* D box essentially eliminates all time delay before cell cycle Start following division, even in very small newborn cells. *CLB3Δdb* cells show no cell cycle arrest response to mating pheromone, and *CLB3Δdb* completely bypasses the requirement for *CLN* G₁ cyclins, even in the absence of the early expressed B-type cyclins *CLB5,6*. Thus, regulated mitotic proteolysis of Clb3 is specifically required to make passage of Start in the succeeding cell cycle “memoryless”—dependent on conditions within that cycle, and independent of events such as B-type cyclin accumulation that occurred in the preceding cycle.

KEYWORDS Clb3; destruction box; mitotic exit; G₁ cyclin control; Start

THE eukaryotic cell cycle is regulated by cyclin-dependent kinases (CDKs) bound to cyclins (Bloom and Cross 2007). In *Saccharomyces cerevisiae*, the *Cdc28* CDK binds to nine cyclins: G₁ cyclins *Cln1-3*; S phase B-type cyclins *Clb5,6*; and mitotic cyclins *Clb1-4*. These cyclins have sharply different biological functions: *cln1,2,3* null strains have an absolute defect in cell cycle initiation (“Start”) but no defect in any post-Start events (DNA replication, spindle assembly, nuclear division, and cytokinesis) (Richardson *et al.* 1989; Cross 1990). In contrast, *clb1,2,3,4* null strains execute Start and DNA replication, but fail to execute cell division (Fitch *et al.* 1992; Richardson *et al.* 1992).

Specificity of cyclin function can derive from differential regulation at many levels: cyclin abundance or subcellular localization, response to inhibitors, degree of activation of *Cdc28* kinase activity, and cyclin-specific substrate targeting by docking motifs (Loog and Morgan 2005; Bloom and Cross

2007; Kõivomägi *et al.* 2011). These diverse controls may be coordinated to regulate the overall temporal pattern of specific CDK activity. On the other hand, deletion of many cyclin genes leads to, at most, minor defects. Thus, cyclin specificity is a strong, but not absolute, determinant of function (Roberts 1999; Bloom and Cross 2007).

B-type cyclins are essential for entry into mitosis; subsequent mitotic exit (cytokinesis, telophase, and resetting the system to G₁ in newborn cells) requires mitotic cyclin degradation (Murray and Kirschner 1989; Murray *et al.* 1989; King *et al.* 1996). Degradation requires cyclin ubiquitination by the anaphase-promoting complex (APC), targeted by the cyclin destruction box (D box) or KEN box motifs (Glotzer *et al.* 1991; Pflieger and Kirschner 2000). Consistent with the requirement for mitotic cyclin degradation for mitotic exit, precise genomic removal of the D box and KEN boxes from the budding yeast mitotic cyclin *Clb2* caused a first-cycle block to mitotic exit (Wäsch and Cross 2002).

The ability of mitotic B-type cyclins to both induce mitotic entry and block mitotic exit may tightly couple many aspects of cell cycle progression to once-per-CDK-cycle (Nasmyth 1996). As B-type cyclin-CDK activity rises, mitotic entry is induced,

Copyright © 2016 by the Genetics Society of America
doi: 10.1534/genetics.116.194837

Manuscript received August 16, 2016; accepted for publication October 25, 2016; published Early Online October 28, 2016.

¹Corresponding author: The Rockefeller University, 1230 York Ave., New York, NY 10065. E-mail: fcross@rockefeller.edu

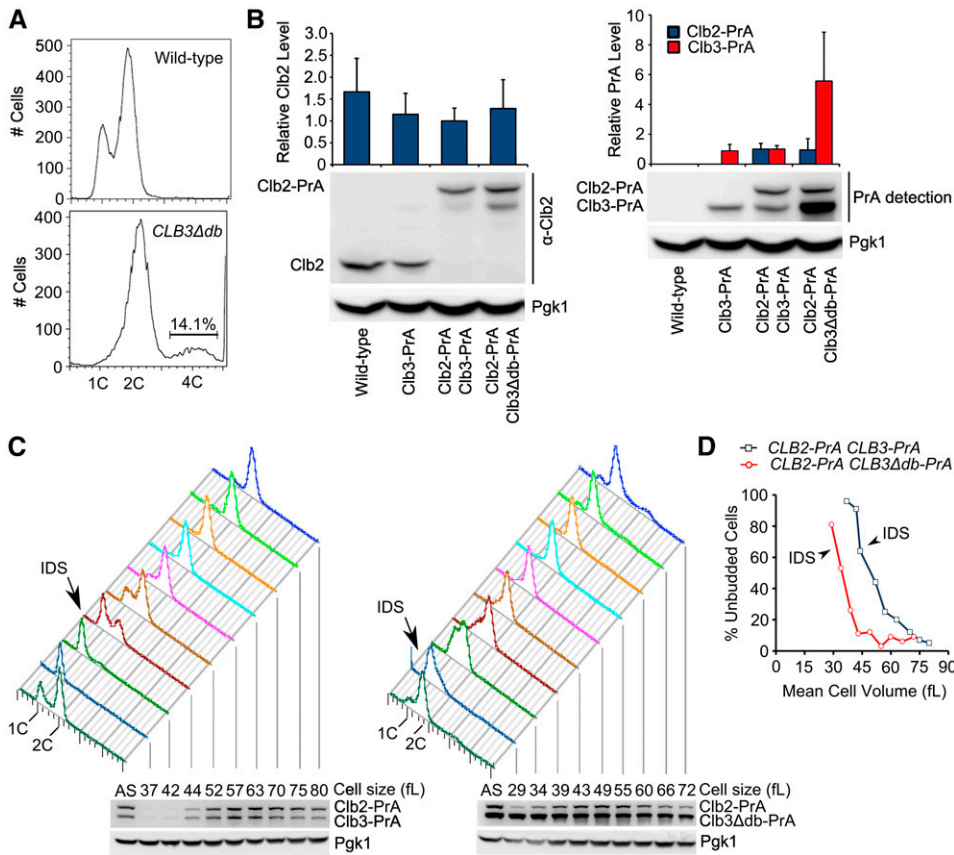


Figure 1 DNA content and protein abundance in asynchronous and elutriated cultures of *CLB3Δdb* cells. (A) Representative FACS profiles of wild-type and *CLB3Δdb* strains in log-phase asynchronous culture. (B) Clb2 and Protein A immunoblots from asynchronous cultures of Clb3-PrA Clb2-PrA and Clb3Δdb-PrA Clb2-PrA strains (standardized to Pgk1, then to PrA signal in Clb3-PrA Clb2-PrA strain). Error bars are SD from two parallel Western blots with the same strains. (C) DNA content and Protein A level in elutriation fractions of Clb3-PrA Clb2-PrA and Clb3Δdb-PrA Clb2-PrA strains. DNA content was determined by flow cytometric analysis. Protein levels in elutriation fractions, as shown in the immunoblot, were normalized to Pgk1. The first sample in FACS profiles and immunoblot (denoted by “AS”) is from asynchronous culture taken immediately before fractionation by elutriator. (D) Percent unbudded cells vs. mean cell volume in each elutriation fraction. Percentage of unbudded cells was determined by visual microscopic examination of a subset of each fraction (~200 cells). Mean cell volume was measured by Coulter cell size analyzer. IDS, Initiation of DNA synthesis [as determined by flow cytometric analysis of DNA content; shown in (C)].

but exit is suppressed; upon B-type cyclin degradation, no further mitotic entry events occur, but mitotic exit is allowed (Nasmyth 1996). Systematic variation in “locked” levels of the Clb2 mitotic cyclin led to the need to revise this “ratchet” model to include a key role for the regulated Cdc14 phosphatase (Drapkin *et al.* 2009). Cdc14 activation, in turn, is under partially autonomous oscillatory control, requiring a mechanism for oscillator coordination (Lu and Cross 2010).

The *CLB1/2* and *CLB3/4* gene pairs are highly similar, but the *CLB3/4* vs. *CLB1/2* divergence is ancient (Archambault *et al.* 2005). Of *CLB1-4*, *clb2* deletion led to the most extreme phenotypes; *CLB3* has mitotic functions partially overlapping with *CLB2* (Fitch *et al.* 1992; Richardson *et al.* 1992). Clb3 and Clb2 are similarly abundant through the cell cycle (Cross *et al.* 2002), but differ in activity toward diverse substrates (Köivomägi *et al.* 2011).

Clb3 is degraded upon mitotic exit in parallel with Clb2 (Cross *et al.* 2002). Removal of the Clb2 D box results in failure of mitotic exit and consequent lethality (Wäsch and Cross 2002). Here, we characterize the requirement for the Clb3 D box for proteolytic regulation and for cell cycle control.

Materials and Methods

Strains and plasmids

Standard methods were used for transformation, mating, and tetrad analysis. All strains were derivatives of W303. All

strains with *CLB3Δdb* were generated using HO-induced exact gene replacement of the *CLB3* allele (Cross and Pecani 2011).

Construction of *clb1 clb2 CLB3Δdb* required some more complex procedures. We crossed a *clb1 clb2::GALL-CLB2-URA3 clb6::kanMX* strain with a *MATa^{inc} GAL-HO CLB3Δdb-URA3-CLB3 clb4::HIS3* strain on a YEPD plate to keep *GAL-HO* inactive, then dissected tetrads on galactose medium to simultaneously maintain viability of segregants bearing *clb1 clb2::GALL-CLB2*, and induce cleavage of the *HO* cut site to obtain *CLB3Δdb* recombinants. (*clb6::kanMX* was used in the experiment for technical convenience because of its tight linkage to the unmarked *clb1* deletion; previous findings (Epstein and Cross 1992; Fitch *et al.* 1992; Richardson *et al.* 1992; Schwob and Nasmyth 1993; Cross *et al.* 1999, 2002) make it unlikely that *clb6* deletion has a significant effect on these results.) We identified strains that were *MATa^{inc} GAL-HO CLB3Δdb clb1 clb2::GALL-CLB2 clb6::kanMX* (*clb6* was maintained due to linkage with *clb1*).

Elutriation

Elutriation was carried out in a Beckman J-6M centrifuge at 3000 rpm and 4°. YEPD cultures (1 liter, OD₆₆₀ ≈ 0.4) were collected by filtration, resuspended in 100 ml water, and sonicated in three 1-min intervals at power setting “4” in a Misonix XL2020 sonicator. Cell suspension fractions were collected after 10% increases in pump speed. Half of each cell

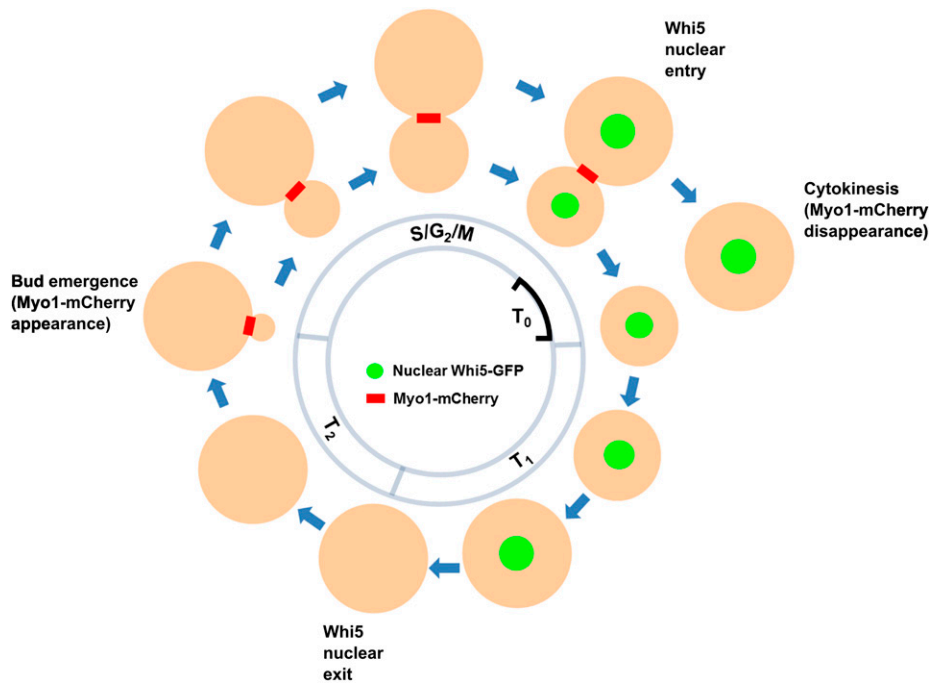


Figure 2 Illustration of cell cycle periods T_0 , T_1 , T_2 , G_1 , and $S/G_2/M$. Periods T_1 and T_2 were defined by Di Talia *et al.* (2007). T_0 is defined in this study as the time between Whi5 nuclear entry and Myo1-mCherry disappearance from the bud neck (as shown).

fraction was fixed with 70% EtOH for subsequent flow cytometric analysis; the other half was used for protein preparation for Western blotting.

Western blotting and kinase activity assays

Western blotting was carried out using standard methods. Anti-Pgk1 (Invitrogen) and anti-Clb2 (Covance) were used at 1:10,000 dilution. Peroxidase anti-peroxidase complex (Sigma P1291) for detection of Protein A-tagged proteins was used at 1:5000 dilution. Anti-mouse and anti-rabbit secondary antibodies (GE) were used at 1:5000 dilution.

For kinase activity assays, cells were washed once in LSHN (50 mM NaCl, 10 mM HEPES pH 7.5, 10% Glycerol). Glass beads (400 μ l) and 400 μ l LSHNN (LSHN + 0.1% NP-40) with protease and phosphatase inhibitors were added, and cells were broken with a FastPrep FP120 Cell Disruptor (Thermo Electron Corp.) in two 20 sec intervals at setting 5. Cell lysates were centrifuged for 2 min, and the supernatant was incubated with 30 μ l Rabbit IgG-Agarose beads (Sigma A2909) for 1 hr at 4°. Bound beads were washed four times with LSHNN, once with HNN (250 mM NaCl, 10 mM HEPES pH 7.5, 10% Glycerol, 0.1% NP-40), once with kinase buffer (10 mM HEPES pH 7.5, 10 mM $MgCl_2$, 1 mM DTT), and resuspended in 60 μ l kinase buffer. The kinase activity assay was carried out essentially as described by Levine *et al.* (1996). Histone H1 radioactivity was detected using a Typhoon 9400 variable imager (Amersham Biosciences). Both Western blot and kinase activity images were quantitated using ImageJ software (Schneider *et al.* 2012; Schindelin *et al.* 2015).

Time-lapse and fixed cell microscopy

Time-lapse and fixed cell microscopy were carried out essentially as previously described (Di Talia *et al.* 2007;

Oikonomou and Cross 2011; Rahi *et al.* 2016). Fixed cell images were acquired with Micro-Manager software (Edelstein *et al.* 2010, 2014). The flow cell experiments were performed using the ONIX Microfluidic Perfusion System (CellASIC) with a Leica DMI6000B inverted fluorescence microscope. Cell segmentation and quantification were carried out with custom Matlab software as in Rahi *et al.* (2016).

Flow cytometry and cell size measurements

For flow cytometry measurements, cells were fixed in 70% ethanol, stained with propidium iodide (PI), and analyzed as described (Epstein and Cross 1992) using a BD FACSCalibur, or a BD Accuri C6 instrument (Becton Dickinson). Cell size was measured using a Z2 Coulter Cell and Particle Counter (Beckman Coulter), and analyzed with Z2 AccuComp software (Beckman Coulter).

Data availability

The authors state that all data necessary for confirming the conclusions presented in the article are represented fully within the article. Strains and data used in this study are available upon request.

Results

The Clb3 D box is not required for cell cycle progression

All mitotic cyclins in *S. cerevisiae* contain a nine amino acid D box, which serves as a target for ubiquitination and subsequent proteolysis toward the end of mitosis (Glotzer *et al.* 1991; Fitch *et al.* 1992; Richardson *et al.* 1992). Removal of the D box from *CLB2* effectively prevents Clb2 degradation

Table 1 Cell cycle timing in daughter cells

Strain	T ₀ (min)	T ₁ (min)	T ₂ (min)	S/G ₂ /M (min)
Wild type	6 ± 2 (50)	19 ± 10 (50)	17 ± 9 (50)	53 ± 8 (50)
<i>CLB3Δdb</i>	6 ± 2 (50)	0 ± 1 (50)	18 ± 10 (50)	71 ± 16 (50)

Times are mean ± SD. Number of cells scored in parentheses. We define T₀ as the time from *Whi5* entry to cytokinesis (*Myo1* ring disappearance) (Figure 2); T₁, time from *Myo1* ring disappearance to *Whi5* exit; T₂, time from *Whi5* exit to bud emergence (Di Talia *et al.* 2007); S/G₂/M, time from *Myo1* ring appearance at incipient bud neck to disappearance at cytokinesis. The frame resolution was 3 min.

(Wäsch and Cross 2002). *CLB2Δdb* cells are not viable without overexpression of the *Clb*-CDK inhibitor *Sic1*. Turning off *SIC1* expression in *CLB2Δdb GAL-SIC1* strains leads to arrest at mitotic exit: long mitotic spindles with separated chromosomes, without cytokinesis or rereplication of DNA (Wäsch and Cross 2002).

Clb3 and *Clb2* overlap functionally (see *Introduction*); also, *Clb3* and *Clb2* oscillate nearly in phase in wild-type cells, and have similar abundance (Cross *et al.* 2002). Thus, removal of the D box from *CLB3* could have similar results as with *CLB2*. We employed *GAL-HO* mediated exact gene replacement in a novel method to construct an exact endogenous replacement of the wild-type *CLB3* allele with an allele lacking the D box sequence RVALSRVTN (Cross and Pecani 2011). This method allows recovery of *CLB3Δdb* or *CLB3* in individual cells (depending on crossover point) without selection, and efficiently detects lethal recombinants. Contrary to expectation, fully viable recombinants bearing the *CLB3Δdb* allele were readily recovered. Here, we characterize the phenotype of these cells.

DNA flow cytometry profiles from asynchronous *CLB3Δdb* cultures are depleted of 1C DNA and enriched for 4C (Figure 1A). However, microscopy showed that the average number of nuclei per cell body (mother or bud), was about 0.67 for both wild type and *CLB3Δdb*, indicating normal coordination of budding and nuclear division. In the *CLB3Δdb* population, aberrant cells with >2 cell bodies were observed with frequency similar to the 4C FACS signal (13% vs. 14%). Therefore, *CLB3Δdb* likely causes a delay in cytokinesis or cell separation. If both daughter nuclei in a conjoined pair replicated DNA, 1C cells would be rare, and replication would result in a 4C FACS signal. Since most cells are 2C, any such delay must be transient.

To test for cytokinesis delay, we measured the time of *Myo1* disappearance relative to *Whi5* nuclear entry. *Myo1* forms a ring at the bud neck, which disappears at the completion of cytokinesis (Bi *et al.* 1998); the *Whi5* transcriptional repressor enters the nucleus 6 min before disappearance of the *Myo1* ring (Figure 2; Di Talia *et al.* 2007). We confirmed this measurement, and found it to be identical in *CLB3* and in *CLB3Δdb* cells (Table 1, T₀). Therefore, the 4C peak in *CLB3Δdb* FACS is likely due to a transient delay in cell separation after cytokinesis. This delay will reduce the 1C population, and increase 4C, if replication completes before cell separation.

The *Clb3* D box regulates *Clb3* protein abundance

To determine if the *Clb3* D box was required for cell-cycle-dependent *Clb3* proteolysis, we employed the same gene

replacement method in a strain containing a C-terminal Protein A epitope tag on the endogenous *CLB3* [PrA-tagged *Clb3* is fully functional (Cross *et al.* 2002)]. We then compared protein abundance of endogenously expressed *Clb3*-PrA to *Clb3Δdb*-PrA. We detected Protein A with IgG, and *Clb2* with specific antibodies, in extracts from asynchronous cultures of *CLB3Δdb*-PrA *CLB2*-PrA, *CLB3*-PrA *CLB2*-PrA, *CLB3*-PrA, and *CLB2 CLB3* strains (Figure 1B). *Clb3*-PrA and *Clb2*-PrA migrate to different gel positions and can be detected simultaneously by PrA detection, allowing direct comparison of *Clb2* and *Clb3* levels in doubly tagged cells (Cross *et al.* 2002). *Clb3*-PrA and *Clb2*-PrA levels were comparable (Figure 1B, this study; Cross *et al.* 2002). *Clb3Δdb*-PrA abundance, however, was almost sixfold higher than *Clb3*-PrA or *Clb2*-PrA (Figure 1B). To follow *Clb3Δdb* levels through the cell cycle, we fractionated cells according to cell size by elutriating log-phase *CLB3Δdb*-PrA *CLB2*-PrA and *CLB3*-PrA *CLB2*-PrA cultures (Figure 1C). Small newborn G₁ cells contain almost no *Clb2* or *Clb3*, which accumulate in parallel with respect to time of DNA replication and budding. In contrast, *Clb3Δdb*-PrA is present throughout the cell cycle at a level ~3- to 10-fold higher than the peak level of *Clb2*-PrA. This defect in regulation of *Clb3*-PrA levels was not due to global failure of cyclin proteolysis, since *Clb2*-PrA in the same cells was degraded approximately normally.

In both *CLB3*-PrA and *CLB3Δdb*-PrA elutriated cultures, the smallest cells had 1C DNA content, with increasing proportions of 2C observed in progressively larger cell fractions. *CLB3Δdb*-PrA cultures showed 2C cells in fractions collected at significantly smaller cell size than *CLB3*-PrA, indicating initiation of DNA replication at smaller cell size in *CLB3Δdb*-PrA cells. Essentially identical results were obtained in a repeat experiment with the same strains, and in an experiment with strains lacking the Protein A tag (data not shown). *CLB3Δdb* cells (with or without the Protein A tag) also showed budding at significantly smaller cell size than *CLB3* controls (Figure 1D).

The implications of apparent loss of size control over DNA replication and budding in *CLB3Δdb* strains are pursued in more detail below.

Clb3-associated protein kinase activity persists through mitotic exit in the absence of the *Clb3* D box

It was surprising to observe high levels of *Clb3Δdb* apparently persisting throughout the cell cycle, given the ability of undegradable *Clb2* to block mitotic exit (Wäsch and Cross 2002). Both *Clb2* and *Clb3* function by activating the *Cdc28* protein kinase (Bloom and Cross 2007), so we considered the possibility that *Clb3Δdb* might be specifically defective in *Cdc28* activation. *CLB3Δdb*-PrA, and *CLB3*-PrA strains were grown to log-phase, and protein extracts were incubated with IgG beads to purify *Clb3*-PrA complexes. Kinase activity was then assayed by phosphorylation of histone H1 (Figure 3A). Kinase activity in the *CLB3Δdb*-PrA strain was significantly higher than in the *CLB3*-PrA strain (Figure 3A), although this difference was less pronounced than the difference in *Clb3* protein levels (Figure 1B). *Clb3Δdb* could have an intrinsic partial defect in activating

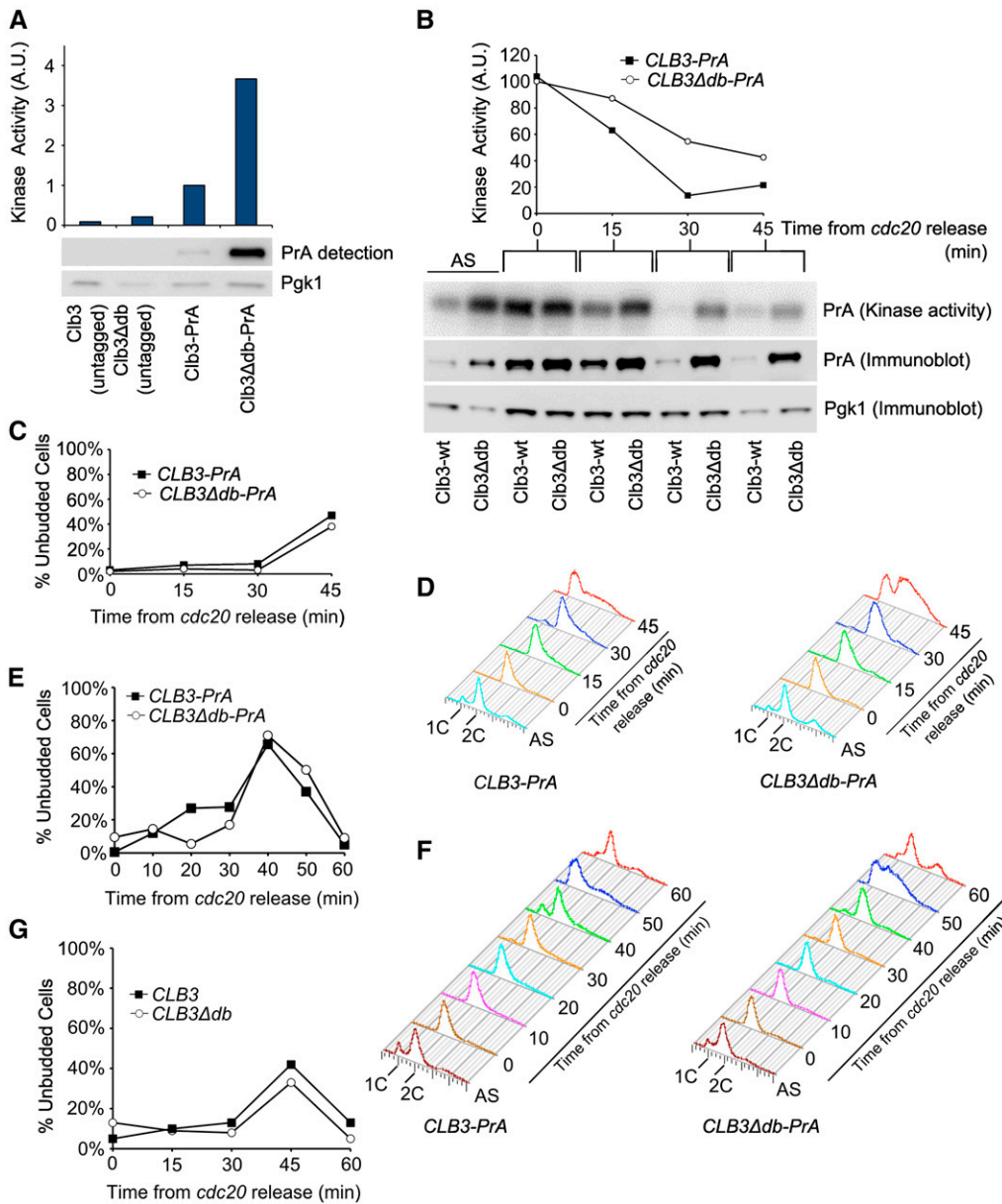


Figure 3 Clb3Δdb-associated kinase activity, DNA content, and budding in asynchronous cultures, and after release from *MET-CDC20* block. (A) Kinase activity in IgG pull-downs from asynchronous cultures. (B) Kinase activity in IgG pull-downs from *MET-CDC20* block/release time-course with *CLB3-PrA* and *CLB3Δdb-PrA* strains. Immunoblot is from total cell lysate before IgG pull-down. (C) Percent unbudded cells following *cdc20* release [same strains as in (B)]. Percentage of unbudded cells was determined by visual microscopic examination of a subset (~200 cells) of samples taken at each timepoint. (D) DNA content in same samples as in (B), as measured by flow cytometric analysis. (E) Timecourse in (B), (C), (D) was repeated with 10 min timepoints to more accurately determine division time. (F) DNA content, as measured by flow cytometric analysis, is also shown for the repeat timecourse in (E). (G) Percent unbudded cells following *cdc20* release in strains without the PrA tag.

Cdc28; alternatively, high levels of Clb3Δdb might result in limitation for free *Cdc28* or other components. *Cdc28* is present in excess of cyclins (Cross *et al.* 2002), but not by a large factor, so *Cdc28* may be limiting in *CLB3Δdb* cells.

If Clb3Δdb or its associated kinase activity was low specifically during mitotic exit, this could result in viability of *CLB3Δdb* cells despite these cells containing high levels of Clb3Δdb-associated kinase activity through most of the cell cycle. To examine Clb3Δdb levels, and associated kinase activity, specifically during exit from mitosis, we introduced *CLB3Δdb-PrA* and *CLB3-PrA* into a *MET-CDC20* background. *MET-CDC20* places the essential APC activator *Cdc20* under methionine control, allowing a rapidly reversible block to mitotic exit (Yeong *et al.* 2000). Methionine was added to log-phase cultures to turn off *MET-CDC20* expression and block cells in metaphase, then methionine was removed to

release the block (Figure 3, B–G). Clb3 protein and associated kinase activity were comparably high at the block in *CLB3-PrA* and *CLB3Δdb-PrA* strains (Figure 3B). After release, both declined sharply in the *CLB3-PrA* strain. Although kinase activity in the *CLB3Δdb-PrA* strains decreased by 50% 45 min after the release from *MET-CDC20* block, it was significantly higher than in the *CLB3-PrA* strain throughout the time-course, and about half the level in *CLB3-PrA* at the *cdc20* block [which is very likely elevated significantly over the normal peak level due to continued synthesis without degradation (Drapkin *et al.* 2009)]. Despite persistence of substantial Clb3Δdb-associated kinase activity after release of the *cdc20* block, cell division (indicated by accumulation of unbudded cells; Figure 3C) was nearly identical in *CLB3Δdb-PrA* and *CLB3-PrA* strains. This result was confirmed in strains without the PrA tag (Figure 3G).

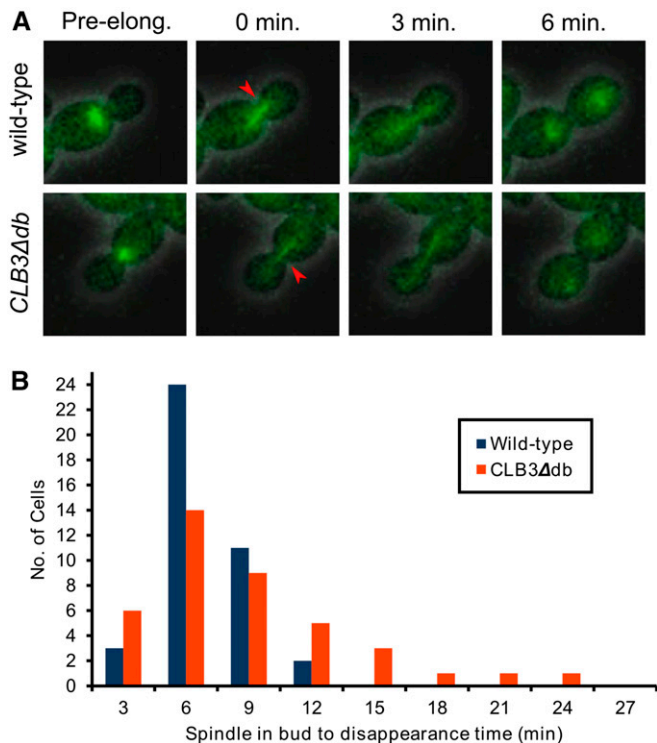


Figure 4 Measurement of anaphase length in wild-type and *CLB3Δdb* cells using time-lapse microscopy. (A) Representative *TUB1-GFP* images. Length of anaphase was scored as entry of spindle into the bud (A_E) to spindle disappearance (A_D). Red arrows indicate newly formed spindle. (B) Distribution of anaphase times (A_E to A_D) in wild-type and *CLB3Δdb* cells.

In the *CLB3-PrA* strain, accumulation of unbudded cells was associated with transition from a uniform 2C FACS peak to accumulation of mostly cells with 1C DNA content; subsequently this 1C peak transitioned to 2C, consistent with DNA replication in the succeeding cell cycle (Figure 3, C and D). This picture was less clear in the *CLB3Δdb-PrA* strain, where a significant 2C population was present at all time points (also apparent in the longer time-course; Figure 3F). This could have indicated some mitotic delay; however, the same cell populations showed almost exactly comparable cell division and rebudding as wild type, as indicated by the proportion of unbudded cells (Figure 3C). The lack of strong accumulation of a 1C peak is likely due to a very short G_1 period, consistent with the analysis of elutriated asynchronous cultures above (Figure 1, C and D), and with the analysis of *Whi5* nuclear residence times below (Figure 7 and Figure 8).

To detect possible mitotic delay at the single-cell level, specifically during anaphase and telophase, we used time-lapse microscopy of log-phase *CLB3Δdb* and *CLB3* strains with GFP-tagged tubulin (*TUB1-GFP*). We recorded the time from spindle entry into the bud (A_E) to its disappearance (A_D) as an estimate for the length of anaphase. Average A_E to A_D time was ~7 min in wild-type and ~9 min in *CLB3Δdb* cells (Figure 4). There was, however, much more variability in A_E to A_D times in *CLB3Δdb* cells compared to wild type, with *CLB3Δdb* cells having more short (3 min) and long (>12 min) anaphase times (Figure 4).

In summary, while the *Clb3* D box is needed to provide regulation of *Clb3* protein and associated kinase activity, absence of this regulation does not impede mitotic exit by more than a short interval.

Fully functional *Cdc14* is required for viability in the absence of the *Clb3* D box

Mitotic exit is likely dependent on the balance of *Clb*-*Cdc28* kinase activity and the antagonistic *Cdc14* phosphatase activity on mitotic targets (Drapkin *et al.* 2009). Mitotic exit can be blocked when relevant targets are kept above a phosphorylation threshold by high *Clb*-*Cdc28* activity, and allowed when *Cdc14* dephosphorylates these targets below the critical threshold (Drapkin *et al.* 2009). If *Clb3Δdb* and *Cdc14* share at least one common target, the dephosphorylation of which is required for mitotic exit, then, according to this model, mitotic exit will only be allowed if the increased kinase activity from *Clb3Δdb* is still not sufficiently high to overcome dephosphorylation of the relevant target(s) by *Cdc14*. If the activity of *Cdc14* is reduced, however, the phosphatase/kinase ratio might be decreased enough to bring the phosphorylation of the relevant target(s) above the threshold required for mitotic exit, so mitotic exit is blocked.

To test for viability of *CLB3Δdb* cells with lowered *Cdc14* activity, we used the temperature-sensitive allele *cdc14-1* (Hartwell *et al.* 1974), which can be partially rescued at non-permissive temperature by overexpressed *SIC1* (Jaspersen *et al.* 1998; Yuste-Rojas and Cross 2000). We made 10× serial dilutions of *CDC14 CLB3*, *CDC14 CLB3Δdb*, *cdc14-1 CLB3*, and *cdc14-1 CLB3Δdb* cells (all bearing *GAL-SIC1*) on YEP-Glucose (“YEPD”; *GAL* off) and YEP-Galactose (“YEPG”; *GAL* on) plates, and placed them at various temperatures (Figure 5A). Because the product of *cdc14-1* is temperature-sensitive, its activity should decrease with increasing temperature, and it may not be fully functional even at permissive temperature.

Viability of *GAL-SIC1 CDC14 CLB3* and *GAL-SIC1 CDC14 CLB3Δdb* cells was unaffected by temperature or growth medium (Figure 5A). *GAL-SIC1 cdc14-1 CLB3* cells were viable up to 30° with *GAL-SIC1* off (YEPD), and were rescued weakly at higher temperatures with *GAL-SIC1* on (YEPG), consistent with previous observations (Jaspersen *et al.* 1998; Yuste-Rojas and Cross 2000). *GAL-SIC1 cdc14-1 CLB3Δdb* cells were inviable at all tested temperatures with *GAL-SIC1* off, and were rescued with *GAL-SIC1* on up to 27° (with partial rescue at 30°).

To determine whether the inviability of *cdc14-1 CLB3Δdb* cells is due to arrest at mitotic exit, we cultured the strains above in liquid YEPG medium at 23°, shifted to YEPD to turn off *GAL-SIC1*, and measured DNA content after 3 hr (Figure 5B). *cdc14-1 CLB3Δdb* cells mostly had 2C DNA, and the 4C peak characteristic of *CLB3Δdb* cells was not present, suggesting that these cells replicated DNA once, arrested at mitotic exit, and did not rereplicate DNA. Microscopic examination of the cells used for flow cytometry revealed that nearly all *cdc14-1 CLB3Δdb* cells were large-budded, with two separated nuclei and no rebudding, consistent with

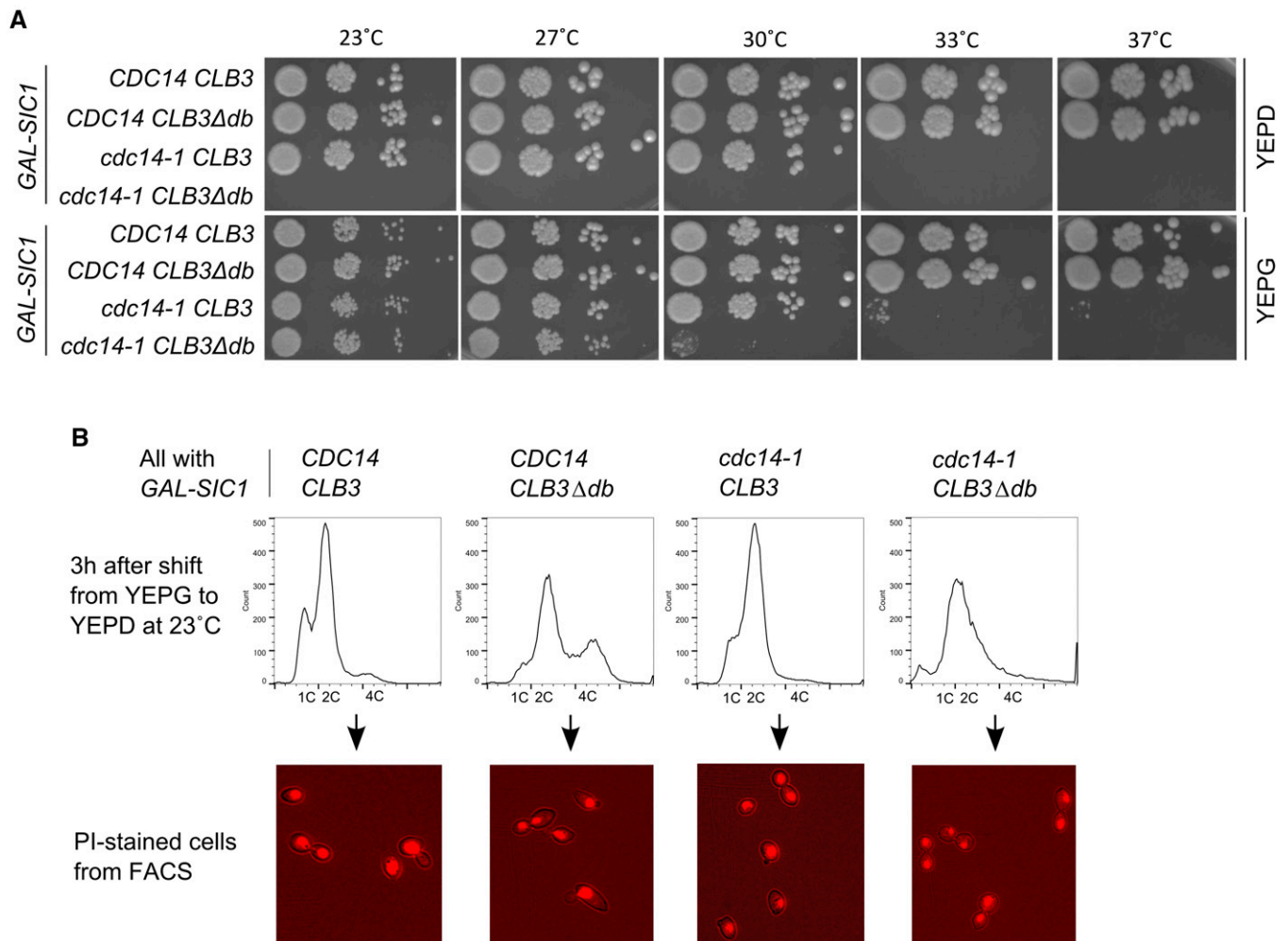


Figure 5 Characterization of *cdc14-1 CLB3Δdb* cells. (A) 10× serial dilutions of *CDC14 CLB3*, *CDC14 CLB3Δdb*, *cdc14-1 CLB3*, and *cdc14-1 CLB3Δdb* cells (all with *GAL-SIC1*) on YEP-Glucose ("YEPD"; GAL off) and YEP-Galactose ("YEPG"; GAL on) plates at various temperatures. (B) Top: DNA content measured 3 hr after shift from YEPG to YEPD medium at 23° (*GAL-SIC1* off). Bottom: microscopic images of cells used for flow cytometry. Nuclei stained with PI.

blocked mitotic exit, whereas the *CDC14 CLB3*, *CDC14 CLB3Δdb*, and *cdc14-1 CLB3* populations were a mixture of cells with single or double nuclei, consistent with continued cycling.

Therefore, it is likely that, with fully functional *Cdc14*, *Clb3Δdb* kinase activity is not high enough to keep relevant targets above the phosphorylation threshold needed to block mitotic exit. With lowered *Cdc14* activity in the *cdc14-1* mutant, the phosphatase/kinase ratio could be reduced enough to bring the phosphorylation of those targets above threshold, blocking mitotic exit.

It is notable that *cdc14-1 CLB3Δdb* cells are completely inviable even at 23°, while *cdc14-1 CLB3* cells are fully viable up to 30°. Thus, *CLB3Δdb* does not block mitotic exit in a *CDC14-wt* background, but it makes the mitotic exit control system much less robust to normally inconsequential reductions in *Cdc14* activity. *SIC1* overexpression probably lowers *Clb3Δdb*-associated kinase activity, rebalancing the system, and allowing mitotic exit. *SIC1* overexpression has very little effect at any temperature on *cdc14-1 CLB3* cell viability.

***Swe1*, *Sic1*, and *Swi5* are not essential for viability in the absence of the *Clb3 D* box**

The experiments above might not detect a brief window of inhibition of *Clb3Δdb*-associated kinase activity. If such a drop were essential for mitotic exit, then a normally non-essential *Clb3* inhibitor might be essential in a *CLB3Δdb* background. We tested the known inhibitors of *Clb-Cdc28*: *Sic1* (a stoichiometric inhibitor), *Swi5* (the major *SIC1* transcription factor), and *Swe1* (a protein kinase that phosphorylates and inhibits *Clb-Cdc28* complexes) (Booher *et al.* 1993; Mendenhall 1993; Schwob *et al.* 1994; Knapp *et al.* 1996; Toyn *et al.* 1997). We made *CLB3Δdb* and *CLB3* alleles using *GAL-HO*-mediated exact gene replacement in *swe1*, *sic1*, or *swi5* backgrounds. Microscopic observation of *CLB3Δdb* recombinants in *swe1*, *sic1*, or *swi5* backgrounds showed no obvious defects compared to isogenic *CLB3* strains (Figure 6A).

Therefore, *Swe1*, *Sic1*, and *Swi5* have no essential role in maintaining viability of *CLB3Δdb* cells. Combined with direct

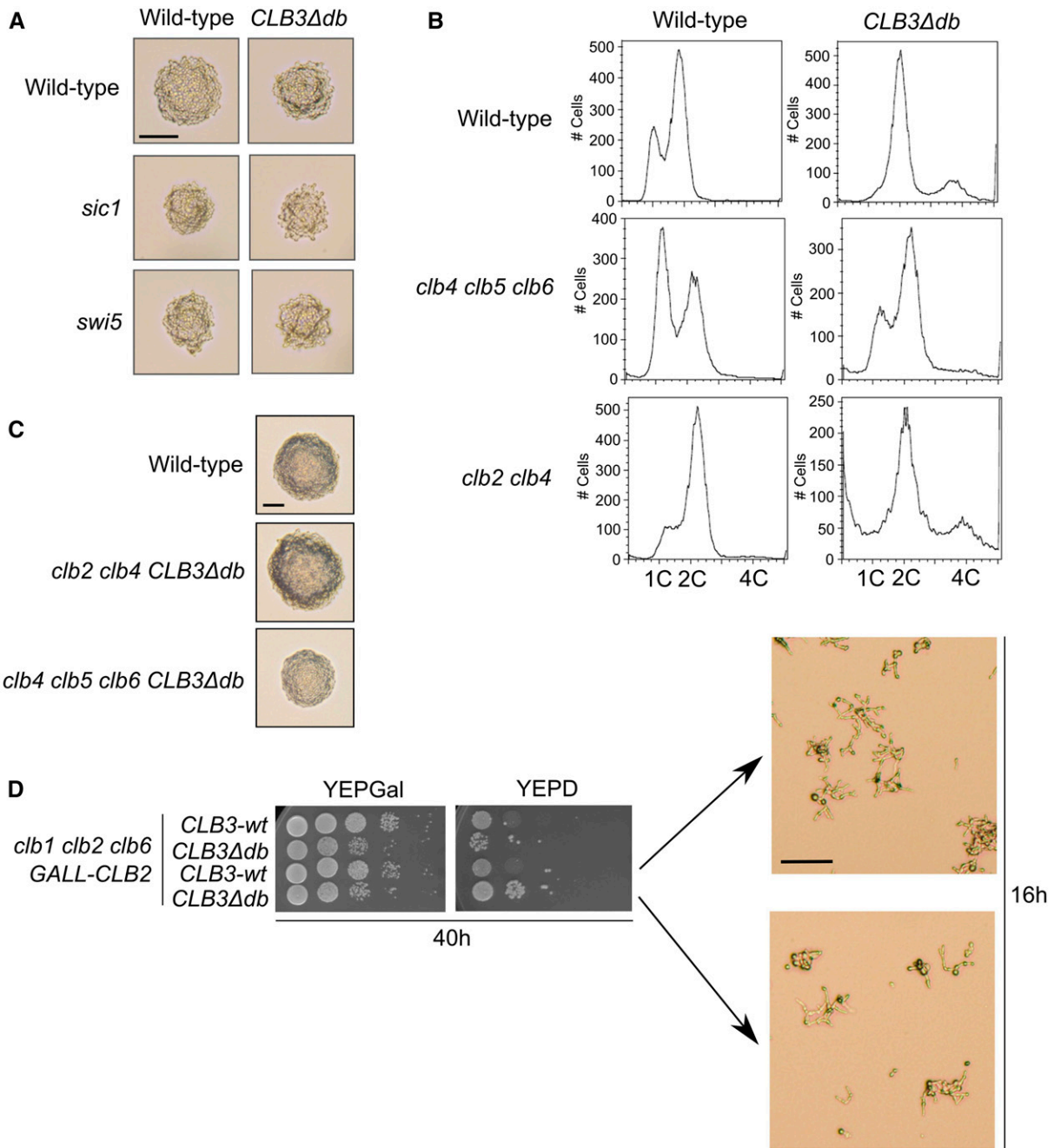


Figure 6 Analysis of Clb3Δdb function in mitosis, and testing for essential Clb-CDK inhibitors in a *CLB3Δdb* background. (A) *CLB3Δdb/wt* strains with and without *sic1* or *swi5* deletions. Images were taken 24 hr after induction of HO site cleavage. Bar, 50 μm. (B) FACS profiles of *CLB3Δdb/wt* strains in either *clb2 clb4* or *clb4 clb5 clb6* backgrounds. (C) *CLB3Δdb/wt* strains in either *clb2 clb4* or *clb4 clb5 clb6* backgrounds 24 hr after induction of HO site cleavage. Bar, 50 μm. (D) Serial dilutions of *clb1 clb2::GALL-CLB2 CLB3Δdb* cells after 40 hr on YEPD to shut off *GALL-CLB2*. Bar, 50 μm.

measurements of protein abundance and associated kinase activity, these observations suggest that even superphysiological levels of undegradable, active Clb3 are essentially fully permissive for mitotic exit.

The Clb3 D box is not required for normal Clb3 functions

We tested genetic function of Clb3Δdb, by introducing *CLB3Δdb* into backgrounds (*clb2 clb4* or *clb4 clb5 clb6*) where Clb3 is essential (Epstein and Cross 1992; Fitch *et al.* 1992;

Richardson *et al.* 1992; Schwob and Nasmyth 1993). Both the *clb2 clb4 CLB3Δdb* and *clb4 clb5 clb6 CLB3Δdb* strains were fully viable (Figure 6C), indicating that Clb3Δdb can carry out normal Clb3 functions.

clb5 clb6 strains bud on schedule, but exhibit a pronounced delay in S phase initiation; this is because normal rapid initiation of DNA replication after Start is dependent on the early expression of Clb5 and Clb6 (Epstein and Cross 1992; Schwob and Nasmyth 1993). In their absence, DNA

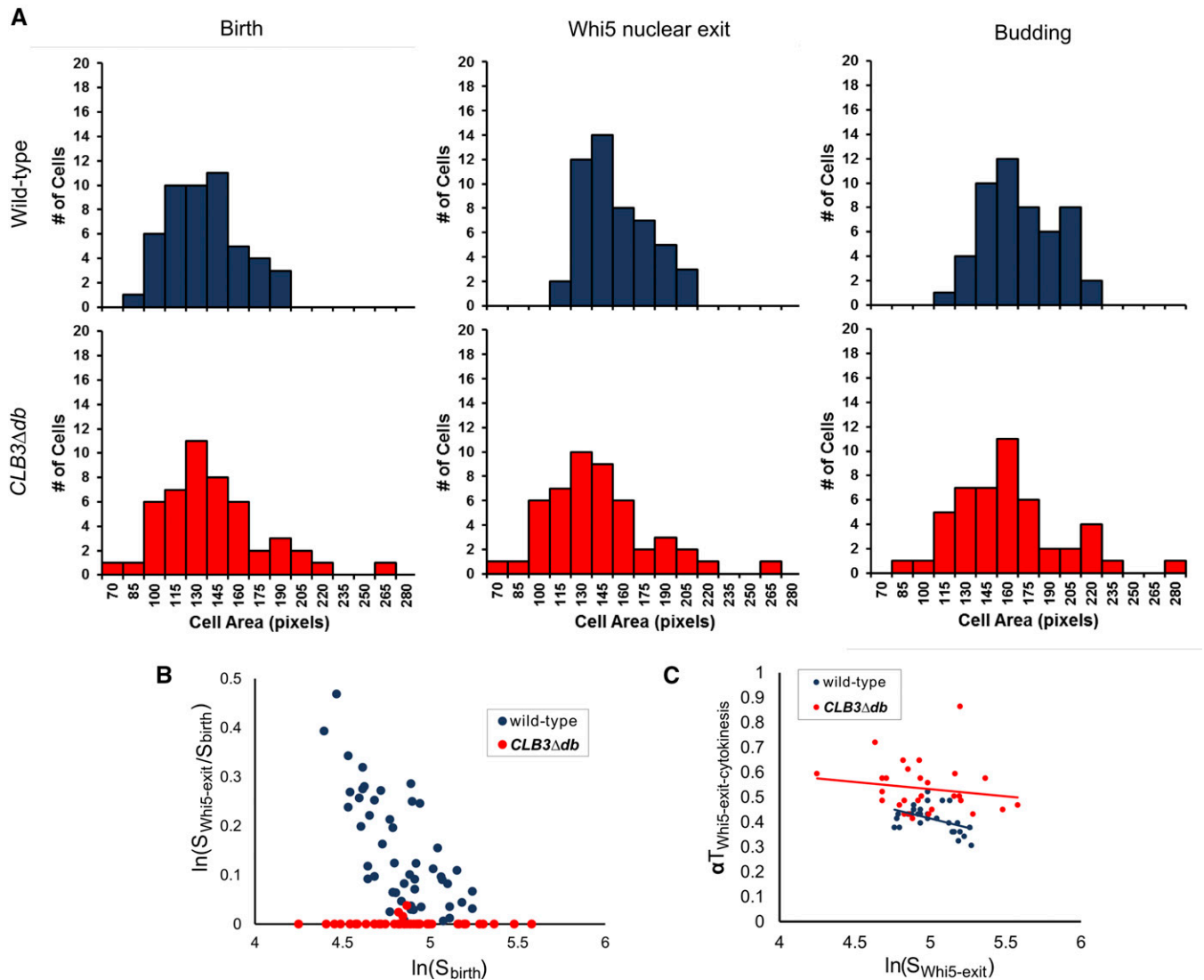


Figure 7 Testing for cell size control in wild-type and *CLB3 Δ db* cells. (A) Distribution of cell areas in wild-type and *CLB3 Δ db* cells at birth, time of Whi5 nuclear exit, and time of budding, as measured from time-lapse microscopy. (B) Log relative growth [$\ln(S_{\text{Whi5-exit}}/S_{\text{birth}})$] vs. log of cell size at birth [$\ln(S_{\text{birth}})$] in wild-type and *CLB3 Δ db* cells. (C) αT (time from Whi5 nuclear exit to cytokinesis multiplied by growth rate) vs. log of cell area at time of Whi5 nuclear exit.

replication initiation is delayed until later expression of *Clb1-4* (Epstein and Cross 1992; Schwob and Nasmyth 1993; Donaldson *et al.* 1998). Confirming this finding, *CLB3 clb4,5,6* mutants exhibit a large accumulation of G_1 cells in asynchronous FACS profiles (Figure 6B); this increase in the G_1 population is almost entirely eliminated in a *CLB3 Δ db clb4,5,6* mutant (Figure 6B), indicating that the stabilized *CLB3 Δ db* is able to promote replication initiation early in the cell cycle. This is consistent with other findings on early replication initiation due to *CLB3 Δ db* (Figure 1 and Figure 3; see above).

clb1 clb2 strains are inviable (Fitch *et al.* 1992; Richardson *et al.* 1992) despite possessing *CLB3*. We wondered whether the high level of *CLB3 Δ db* might allow rescue of a *clb1 clb2* background. We constructed *clb1,2,6 GALL-CLB2* strains that were *CLB3* or *CLB3 Δ db* (see *Materials and Methods*), main-

taining strains on galactose, then examined the effect of shutting off *GALL-CLB2* on glucose medium. Both *clb1,2,6 CLB3* and *clb1,2,6 CLB3 Δ db* cells exhibited rapid arrest as long-budded cells, indicating no rescue of *clb1,2* lethality by *CLB3 Δ db* (Figure 6D). The *clb1 clb2 CLB3 Δ db* population did contain a small fraction of cells with no morphological abnormalities, which formed viable colonies; the nature of this leakage was not investigated. It is clear that in the great majority of cells, *CLB3 Δ db* had no ability to rescue *clb1,2* arrest.

***Clb3* proteolysis may be required for cell size control at Start**

Analysis of elutriated fractions from asynchronous cultures suggested that *CLB3 Δ db* strains bud and initiate DNA replication at a smaller cell size than wild type (Figure 1, C and D),

Table 2 Whi5-GFP nuclear residence times in daughter cells

Strain	Wild Type	<i>CLB3Δdb</i>	<i>sic1Δ</i>	<i>CLB3Δdb sic1Δ</i>
Whi5-GFP in nucleus (min)	25 ± 11 (50)	6 ± 3 (50)	23 ± 14 (50)	0 ± 2 (50)

Times are mean ± SD. Number of cells scored in parentheses.

implying that *Clb3Δdb* promotes both budding and initiation of DNA replication in cells that are below the wild type critical size for these events.

Budding and DNA replication are dependent on the Start transition, which is controlled by the G₁ cyclins *Cln1*, *Cln2*, and *Cln3* (Lew and Reed 1993; Cross 1995; Dirick *et al.* 1995). The Cln regulatory hierarchy starts with *Cln3* inactivating the *Whi5* transcriptional repressor of the G₁/S regulon, which includes *Cln1* and *Cln2* (Costanzo *et al.* 2004; De Bruin *et al.* 2004; Di Talia *et al.* 2007; Skotheim *et al.* 2008). Initial, partial *Whi5* inactivation is followed by rapid completion of *Whi5* inactivation by *Cln1* and *Cln2*, in a transcriptional positive feedback loop (Skotheim *et al.* 2008). Cell size control is coupled to the *Cln3-Whi5* part of this regulatory hierarchy (Di Talia *et al.* 2007): small cells, born with a high *Whi5* concentration, must increase cellular volume to decrease *Whi5* concentration to a critical level that is sensitive to inhibition by *Cln3* (Schmoller *et al.* 2015).

The unbudded interval can be divided into two discrete, independent periods: an initial interval (T₁) during which cells are subject to size control, and a subsequent “timing” interval (T₂) (Di Talia *et al.* 2007). *Whi5* exits the nucleus at the end of T₁ (Figure 2). The Start transition coincides with *Whi5* nuclear exit, when the *Cln1,2* positive feedback loop fires (Di Talia *et al.* 2007; Skotheim *et al.* 2008; Doncic *et al.* 2011). T₁ is longer in small daughter cells since these cells must reach a critical size before progression through Start (Di Talia *et al.* 2007; Schmoller *et al.* 2015).

We used time-lapse microscopy of log-phase *CLB3Δdb* and *CLB3* strains with *MYO1-mCherry* and *WHI5-GFP* to determine the effect of *CLB3Δdb* on cell cycle timing. We restricted our analysis to daughter cells only since there is almost no size control period in mother cells (Di Talia *et al.* 2007). T₁ was eliminated in *CLB3Δdb* daughters, while T₀ (*Whi5* entry to cytokinesis) and T₂ (*Whi5* exit to budding) were unaffected (Table 1). Elimination of T₁ in *CLB3Δdb* cells was compensated by an increase in the interval between bud emergence and cytokinesis, so that the overall division time was unaffected (Table 1).

It is possible that *Whi5-GFP* enters the nucleus briefly during T₀ because of inhibition of *Clb3Δdb* by *Sic1*. To test this, we measured *Whi5-GFP* nuclear residence times in wild-type, *CLB3Δdb*, *sic1Δ*, and *CLB3Δdb sic1Δ* cells (Table 2). We did not detect *Whi5-GFP* nuclear entry in >90% of *CLB3Δdb sic1Δ* daughter cells with a 3 min frame resolution, while the *Whi5-GFP* nuclear residence time in *CLB3 sic1Δ* cells was nearly comparable to that of *CLB3 SIC1*, suggesting that the short interval of *Whi5-GFP* nuclear entry is indeed due to *Sic1* inhibition of *Clb3Δdb*.

Table 3 Daughter cell T₁ and T₂ times with and without *CLN3*

Genotype	T ₁ (min)	T ₂ (min)
Wild type	18 ± 11 (50)	18 ± 7 (50)
<i>CLB3Δdb</i>	0 ± 1 (50)	18 ± 11 (50)
<i>cln3</i>	26 ± 10 (50)	16 ± 7 (50)
<i>cln3 CLB3Δdb</i>	0 ± 1 (50)	18 ± 9 (50)

Times are mean ± SD. Number of cells scored in parentheses. We consider T₁ as time from cytokinesis (estimated as *Whi5* nuclear entry + 6 min) to *Whi5* exit; T₂: time from *Whi5* exit to bud emergence (Di Talia *et al.* 2007).

T₁ is the interval subject to size control (Di Talia *et al.* 2007), so a simple explanation of ablation of T₁ in *CLB3Δdb* cells would be if these cells are born larger than wild-type cells. To test this, we measured distributions of cell sizes at birth (time of *Myo1* ring disappearance) in these movies. Birth sizes were largely overlapping between *CLB3Δdb* and wild-type cells (Figure 7A); however, the distribution of size of *CLB3Δdb* cells was wider, with more extremely small and large cells. Wild-type cell size increased between cell birth and *Whi5* nuclear exit (Figure 7A), reflecting the requirement for cell growth to a critical size for *Whi5* exit. In contrast, since *Whi5* exit was almost immediate upon birth in *CLB3Δdb* cells, there was no change in cell size, even in small newborn cells.

A metric for the degree of size control is derived from a plot of the log of relative growth between birth and *Whi5* exit, vs. log of size at birth (Di Talia *et al.* 2007). Assuming perfect size control, then cell size at *Whi5* exit ($S_{\text{Whi5-exit}}$) is a constant. In this case, a plot of $\ln(S_{\text{Whi5-exit}}/S_{\text{birth}})$ against $\ln(S_{\text{birth}})$ has a slope of -1, with an x-intercept at $\ln(S_{\text{Whi5-exit}})$. Previous measurements resulted in a slope of ~ -0.4 , indicating strong, but imperfect, size control (Di Talia *et al.* 2007). We reproduced this result for wild type (Figure 7B). In contrast, the slope for *CLB3Δdb* cells was essentially 0, indicating absence of detectable size control, even in daughter cells with sizes associated with strong delays in wild type (Figure 7B).

To see if size control is instead shifted to a later phase of the cell cycle in *CLB3Δdb* cells, we plotted αT , the time from *Whi5* exit to *Myo1* ring disappearance (cytokinesis) multiplied by the growth rate, vs. the log of cell size at the time of *Whi5* exit (Figure 7C). If small *CLB3Δdb* cells are delayed in *Myo1* ring disappearance, then αT will be larger for these cells, since their growth rate is comparable. αT showed only moderate dependence on cell size at the time of *Whi5* exit from the nucleus in either wild-type or *CLB3Δdb* cells (Figure 7C); this moderate dependence may provide some level of size control to *CLB3Δdb* cells. We noted above that there is considerable variability in the sizes of *CLB3Δdb* cells, consistent with a global deficit in cell size control.

Deletion of the *CLB3 D* box bypasses Start control by *Cln3 G₁ cyclin*

Cln3, which promotes the nuclear exit of *Whi5*, can control the duration of T₁: deletion or overexpression of *CLN3* prolongs or shortens T₁, respectively (Di Talia *et al.* 2007). Thus, *Clb3Δdb* could eliminate T₁ through hyperactivating *Cln3*, or alternatively by bypassing *Cln3*.

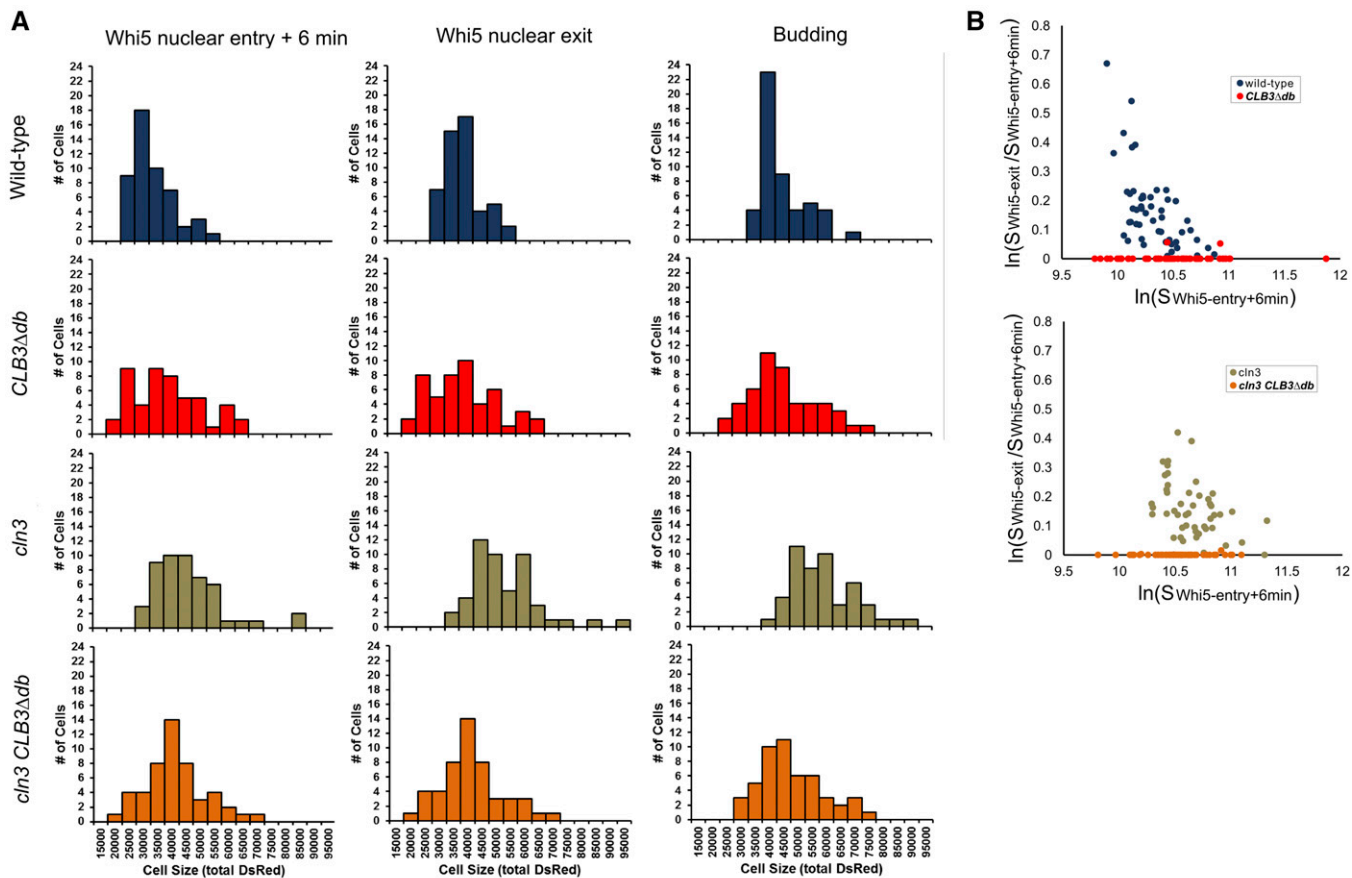


Figure 8 Analysis of cell size control in wild-type, *CLB3Δdb*, *cln3*, and *cln3 CLB3Δdb* cells. (A) Distribution of cell sizes (total DsRed) in wild-type, *CLB3Δdb*, *cln3*, and *cln3 CLB3Δdb* cells at birth (estimated as time of Whi5 nuclear entry + 6 min), time of Whi5 nuclear exit, and time of budding. (B) Log relative growth [$\ln(S_{\text{Whi5-exit}}/S_{\text{Whi5-entry+6min}})$] vs. log of cell size at birth [$\ln(S_{\text{Whi5-entry+6min}})$] in wild-type, *CLB3Δdb*, *cln3*, and *cln3 CLB3Δdb* cells.

To test the dependence of *CLB3Δdb* on *CLN3* for elimination of T_1 , we carried out a similar analysis to that in Figure 7, by time-lapse microscopy of log-phase *CLB3*, *CLB3Δdb*, *cln3*, and *cln3 CLB3Δdb* strains with *WHI5-GFP* and *ACT1pr-DsRed*. In this experiment we used total DsRed signal, since this provides a more accurate estimate of cell size than cell area (Di Talia *et al.* 2007). T_1 was elongated in *cln3 CLB3* cells, as reported (Di Talia *et al.* 2007) but there was no detectable T_1 period in *CLB3db* cells, with or without *CLN3* (Table 3). T_2 remained nearly unchanged between wild type and *CLB3Δdb*, and between *cln3* and *cln3 CLB3Δdb*. Therefore, elimination of T_1 by *Clb3Δdb* is not dependent on *Cln3*.

Deletion of *CLN3* resulted in larger cells, at birth, Whi5 exit, and budding, but this effect was nearly eliminated by *CLB3Δdb* (Figure 8A). The “size control” plot $\ln(S_{\text{Whi5-exit}}/S_{\text{birth}})$ against $\ln(S_{\text{birth}})$ showed readily detectable size control (negative slope) in *CLB3 CLN3*. Size control was also clearly detected in *CLB3 cln3*, but shifted to larger cell size, as reported (Di Talia *et al.* 2007). There was no detectable size control in *CLB3Δdb* cells with or without *CLN3*, even at sizes where *CLB3* cells exhibit clear size control (Figure 8B). These results confirm the findings in Figure 7 obtained using microscopic cell “area,” using instead the *ACT1-DsRed* cell size reporter.

Thus, removal of the *Clb3* D box eliminates pre-Start cell size control independently of *CLN3*, even in very small daughter cells.

In the absence of the *CLB3* D box *G₁/S* cyclins *Cln1,2,3* and *Clb5,6* are no longer required for viability

As shown above, *Clb3Δdb* bypasses the requirement for *Cln3*. The main function of *Cln3* is likely to trigger the *CLN1,2* positive feedback loop (Skotheim *et al.* 2008). We were interested to know whether *Clb3Δdb* could also bypass the need for *Cln1,2*. We constructed *cln1 cln2 cln3 MET3-CLN2* strains that were *CLB3Δdb* or *CLB3*, and grew log-phase cultures on medium lacking methionine to keep *MET3-CLN2*. Methionine was then added to the cultures, and samples of cells were taken every 30 min up to 3 hr to measure DNA content and budding index. Immediately before the addition of methionine, some cells were also placed in 10-fold serial dilutions on solid agar medium with or without methionine (Figure 9A). As expected, the *cln1,2,3 CLB3* strain arrested in the first cell cycle after shutoff of *MET3-CLN2*, accumulating as unbudded cells with unreplicated DNA (Figure 10). In contrast, the *cln1 cln2 cln3 CLB3Δdb* strain exhibited only a partial accumulation of unbudded cells (up to ~40%), and no

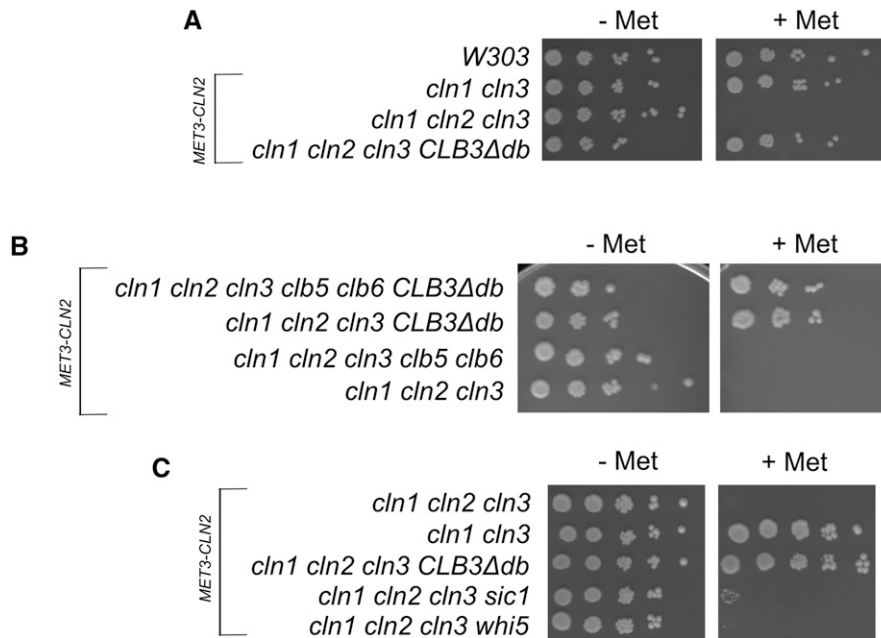


Figure 9 Testing bypass of CLNs and *CLB5/6* in *CLB3Δdb* strains. (A) Serial dilutions of *CLB3Δdb/wt* strains with a *cln1 cln2 cln3 MET3-CLN2* background. Cells were grown to log-phase in medium lacking methionine, then plated in 10-fold serial dilutions on solid medium containing methionine to shut off *MET3-CLN2*. (B) *CLB3Δdb/wt* strains with a *clb5 clb6 cln1 cln2 cln3 MET3-CLN2* background were plated in 10-fold serial dilutions as in (A). (C) *cln-* cells with either wild-type, *CLN2*, *CLB3Δdb*, *sic1*, or *whi5* backgrounds were plated in 10-fold serial dilutions as in (A).

accumulation of cells with unreplicated DNA. This result suggests efficient bypass of the *CLN* requirement. Consistently, serial dilutions on methionine-containing medium show that *cln1 cln2 cln3 CLB3Δdb* cells can form colonies with high efficiency, and an approximately similar growth rate as *CLN*+ wild-type controls (Figure 9A).

Despite their rapid growth rate, microscopic examination of *cln1,2,3 CLB3Δdb MET3-CLN2* colonies grown on +Met revealed significant cell size heterogeneity. To further characterize this, we inoculated *CLB3Δdb cln1 cln2 cln3 MET3-CLN2* cells (pregrown in medium lacking methionine) onto solid medium containing methionine, then separated five individual unbudded or very small budded cells with a microneedle to a fresh area, and examined them microscopically at intervals. All five cells had divided multiple times after 6 hr, forming microcolonies, with some variation in cell size notable. After 24 hr, all five microcolonies had continued to proliferate into a mixture of small and large cells. With the microneedle, we moved the large cells (which were unbudded) to a fresh area of the plate. After another 24 hr, most of these unbudded large cells eventually formed microcolonies again consisting of a mixture of small and large cells. We conclude, therefore, that *CLB3Δdb* effectively bypasses *cln1 cln2 cln3* inviability, but some aspects of the rescue are irregular compared to wild type.

Clb5 and *Clb6* are early expressed B-type cyclins that promote S phase; moderate overexpression of *CLB5* can bypass the *Cln* requirement (Epstein and Cross 1992). However, the bypass of *CLN* deficiency by *Clb3Δdb* is not dependent on *CLB5/6* (Figure 9B).

We showed above that *CLB3Δdb* cells efficiently inactivated *Whi5*. To test whether this could be sufficient to account for *cln1,2,3* bypass by *CLB3Δdb*, we constructed a *cln1,2,3 whi5 MET-CLN2* strain. This strain was completely

inviable on +Met, showing that *CLB3Δdb* has broader Start-promoting activities than just inactivating *Whi5* (Figure 9C). *cln1,2,3* bypass by *CLB3Δdb* is not simply a result of *CLB3Δdb* cells being born with no nuclear *Whi5*.

Comparison of *cln1,2,3* bypass by *CLB3Δdb* and *sic1Δ*

Removing the *Clb3* D box prevents negative control of *Clb3* by the APC (see *Introduction*). Another negative control on B-type cyclins is due to the inhibitor *Sic1*, and deletion of *SIC1* was reported to bypass the *cln1,2,3* requirement (Tyers 1996). To compare the efficiency of *CLN* bypass by *CLB3Δdb* to that of a *sic1* deletion, we made *cln1, cln2, cln3 MET3-CLN2* strains in wild-type, *CLB3Δdb*, and *sic1* backgrounds (with a *cln1 CLN2+ cln3* strain as a positive control) and grew log-phase cultures on medium lacking methionine. The cultures were then plated on YEPD plates (with methionine) to shut off *MET3-CLN2* (Figure 9C). Consistent with the experiment above, *cln1 cln2 cln3* cells quickly arrested as large unbudded cells, but *cln1 cln2 cln3 CLB3Δdb* cells formed microcolonies with similar efficiency and timing as the *cln1 CLN2+ cln3* control. By comparison, the bypass of *cln-* by *sic1* was poor: only ~1% of cells had formed microcolonies after 3 days on the YEPD plate. [*cln1,2,3* bypass seems less efficient in the W303 background than in the experiments of Tyers (1996) in the BF305-15d background; but even in that background, *sic1 cln1 cln2 cln3* cells were large and slow-growing compared to controls (Epstein and Cross 1994; Tyers 1996)].

The *Clb3* D box is required for mating pheromone-induced block to Start

The mating pheromone alpha-factor arrests cells before Start via a signal transduction pathway that inhibits *CLNs* (Peter and Herskowitz 1994; Cross 1995). Given that *Clb3Δdb* bypasses the *cln1,2,3* requirement, we tested whether *CLB3Δdb*

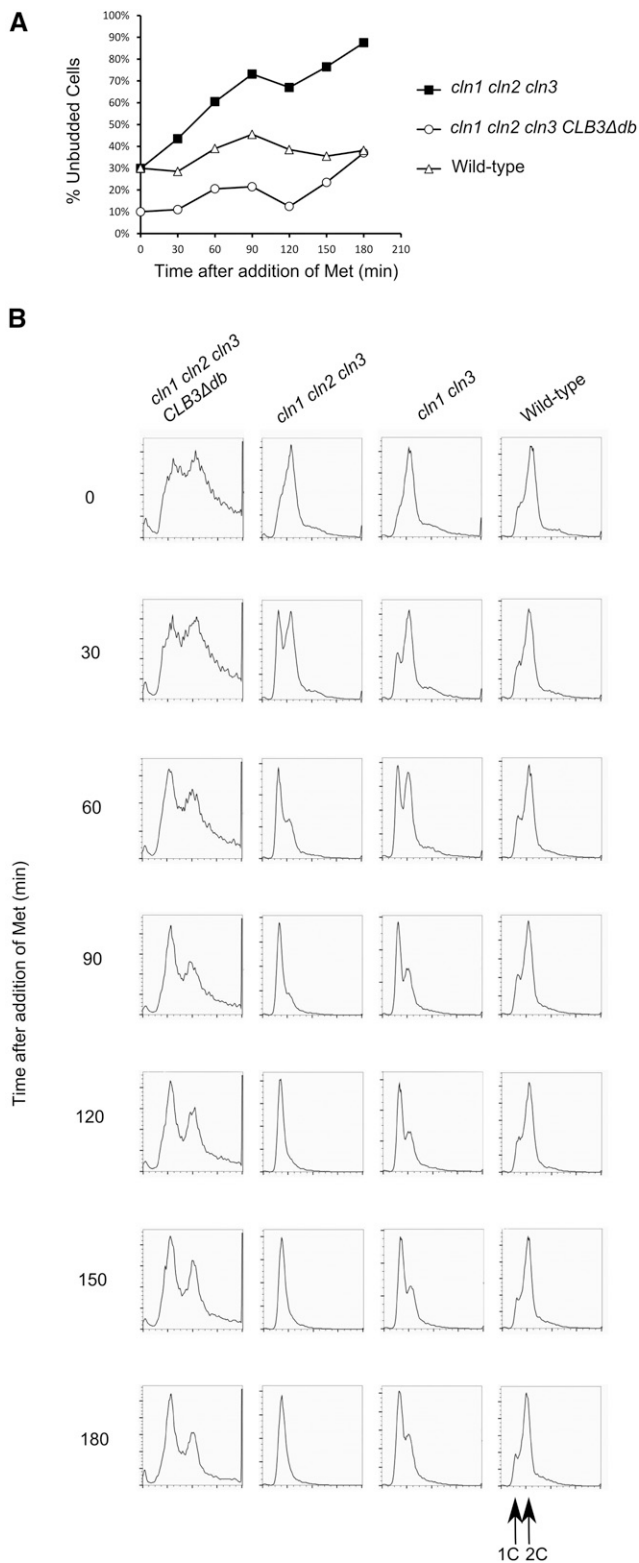


Figure 10 DNA content and budding in *cln1 cln2 cln3 CLB3Δdb* cells after shutoff of *MET3-CLN2*. (A) Percent unbudded cells after block of *MET3-CLN2* by addition of methionine. First sample ($t = 0$) was taken before addition of methionine. (B) DNA content after block of *MET3-CLN2*.

cells were sensitive to mating pheromone. To test for alpha-factor-induced arrest of *CLB3Δdb* cells, we placed log-phase *bar1 CLB3Δdb* and *bar1 CLB3* cells (*MATa*-mating type *bar1*) on a YEPD plate with 10^{-7} M alpha-factor, and checked for arrest after 24 hr. (The *bar1* deletion prevents alpha-factor degradation [Chan and Otte 1982]). All *bar1 CLB3* cells were arrested after 24 hr on alpha-factor, but only ~10% of *bar1 CLB3Δdb* cells were arrested. Therefore, *Clb3* proteolysis is required for effective mating pheromone regulation of Start.

Discussion

Mitotic degradation of *Clb3* is not required for mitotic exit

Destruction box-dependent degradation of mitotic cyclins at the end of mitosis has been proposed to be essential for mitotic exit (Murray and Kirschner 1989; Murray *et al.* 1989; Ghiara *et al.* 1991). Here, we show that *Clb3Δdb*, though functional, stable, and active through the cell cycle, is fully permissive for mitotic exit; the only mitotic defect we noted was a moderate delay in cell separation after cytokinesis. This is unexpected given the significant functional overlap of *CLB3* and *CLB2* (Fitch *et al.* 1992; Richardson *et al.* 1992), and the complete block to mitotic exit imposed by *CLB2Δdb* at the endogenous locus (Wäsch and Cross 2002).

Clb2-Cdc28 may be the most active of the *Clb-Cdc28* complexes, although *Clb2* lacks docking sites possessed by *Clb5* and *Clb3* (Kõivomägi *et al.* 2011). If block of mitotic exit by *Clb2* involves low-affinity substrates not recognized by docking sites (Loog and Morgan 2005; Kõivomägi *et al.* 2011), then perhaps *Clb3*, even at high levels, cannot effectively phosphorylate these targets. This is supported by our observation that deletion of the *Clb3* D box can result in mitotic exit block if *Cdc14* activity is reduced; therefore, *Clb3* likely shares at least one target with *Cdc14*, but could be unable to phosphorylate such a target to levels sufficiently high to block mitotic exit. Components of the mitotic exit network *Cdc15*, *Mob1*, and *Dbf2* have been previously identified as targets of *Clb2-Cdc28* (Jaspersen and Morgan 2000; Ubersax *et al.* 2003; König *et al.* 2010) and could possibly be targets of *Clb3* as well. Indeed, *Mob1* and *Dbf2* have been shown to interact with *Clb3* (Archambault *et al.* 2004).

Absence of mitotic cyclin activity after mitosis is likely required in order to reassemble prereplicative complexes for DNA replication (Dahmann *et al.* 1995; Nasmyth 1996; Detweiler and Li 1998), and to permit budding at the G_1/S phase transition (Lew and Reed 1993; Amon *et al.* 1994). Since both DNA replication and budding occur in *CLB3Δdb* cells, even when present at high levels, *Clb3* may only inefficiently phosphorylate the relevant substrates for these controls as well.

Mitotic degradation of *Clb3* is required to eliminate "memory" of the preceding cell cycle and allow Start control

In contrast to the absence of any significant requirement for *Clb3* proteolysis for mitotic exit, mitotic *Clb3* proteolysis is required for control of Start. Start is conditional on cells

attaining a sufficient cell size; it depends on *Cln3* as an initial upstream signal, and on the *Cln1,2*-dependent positive feedback loop (Cross and Tinkelenberg 1991; Dirick and Nasmyth 1991; Cross 1995; Skotheim *et al.* 2008). Start is also specifically blocked by mating pheromones (Cross 1995). All of these controls are abrogated by removal of the *Clb3* D box: *CLB3Δdb* cells pass Start even when very small, as indicated by the absence of nuclear *Whi5*, and by accelerated budding and DNA replication, in a *Cln3*-independent fashion; *CLB3Δdb* results in mating factor insensitivity, and eliminates the requirement for any of *CLN1,2,3 CLB5,6*. Rescue of *CLN* deficiency by cyclins has been previously reported, but has involved expression of the rescuing cyclins from a strong promoter such as *ADH1* (Koff *et al.* 1991; Léopold and O'Farrell 1991; Lew *et al.* 1991), resulting in gross overexpression of the foreign cyclin. In this study, we have removed only a small regulatory segment of a B-type cyclin expressed under its endogenous promoter. Very efficient *CLN* bypass was observed with mutants in the *CDC28* cyclin-dependent kinase evolved by directed evolution to partial cyclin independence (Levine *et al.* 1999). The mutant *Cdc28* proteins had cyclin-independent kinase activity, which would presumably be present in small newborn cells even after complete mitotic cyclin proteolysis.

The *CLN* gene family has been maintained in almost all members of the large fungal lineage (N. Buchler, personal communication), and the functionally cognate *G₁* cyclins D and E are widespread in animal lineages, although they are also largely dispensable for the core cell cycle (Sicinski *et al.* 1995; Geng *et al.* 2003). Continued selection for presence of *G₁* cyclins is likely due to their role in providing a “starter switch” that allows connection of the cell cycle to regulatory signals, such as cell size in the case of budding yeast. There is an absolute requirement for *CLN* gene expression after cell birth, even in very large newborn cells (Richardson *et al.* 1989; Cross 1990). This means that every cell cycle is effectively memoryless: the firing of the *CLN* switch in the preceding cell cycle is irrelevant. As a consequence, each cell cycle is directly coupled to regulatory systems that target *G₁* cyclins. This is presumably also the reason for the high instability of *Cln* proteins—stabilization of *Cln3* by removing its degradation signal eliminates Start control by mating pheromone and cell size, and previously synthesized stable *Cln3* can promote multiple cell cycles in a *cln1,2,3* background with no further *CLN3* expression (Cross 1990).

Without mitotic destruction, *Clb3* synthesized in the preceding cell cycle may directly activate Start, bypassing the *CLN* regulatory loop. We do not know what phosphorylation targets are responsible for this activity. *Whi5* and *Sic1* are both proposed Cdk targets that restrain Start, but genetic results above show that neither of these targets is sufficient to account for *CLB3Δdb cln*-bypass. Other *Clbs* could have a similar activity if not degraded, although this role is obscured by inhibition of mitotic exit (since exit is a prerequisite for Start). Indeed, Drapkin *et al.* (2009) showed that cells containing a level of *Clb2Δdb* low enough to allow escape of the block to mitotic exit had perturbed regulation of the succeed-

ing Start, since they did not block budding in response to the mating pheromone alpha-factor. The absence of inhibition of mitotic exit by *Clb3Δdb* allows a much clearer view of this new role of mitotic cyclin degradation: blocking memory of the previous cell cycle in newborn cells.

Acknowledgments

We thank all members of the Cross laboratory for insightful discussions. Funding support was from Public Health Service grant 5RO1-GM078153.

Literature Cited

- Amon, A., S. Irniger, and K. Nasmyth, 1994 Closing the cell cycle circle in yeast: G2 cyclin proteolysis initiated at mitosis persists until the activation of G1 cyclins in the next cycle. *Cell* 77: 1037–1050.
- Archambault, V., E. J. Chang, B. J. Drapkin, F. R. Cross, B. T. Chait *et al.*, 2004 Targeted proteomic study of the cyclin-Cdk module. *Mol. Cell* 14: 699–711.
- Archambault, V., N. E. Buchler, G. M. Wilmes, M. D. Jacobson, and F. R. Cross, 2005 Two-faced cyclins with eyes on the targets. *Cell Cycle* 4: 125–130.
- Bi, E., P. Maddox, D. J. Lew, E. D. Salmon, J. N. McMillan *et al.*, 1998 Involvement of an actomyosin contractile ring in *Saccharomyces cerevisiae* cytokinesis. *J. Cell Biol.* 142: 1301–1312.
- Bloom, J., and F. R. Cross, 2007 Multiple levels of cyclin specificity in cell-cycle control. *Nat. Rev. Mol. Cell Biol.* 8: 149–160.
- Booher, R. N., R. J. Deshaies, and M. W. Kirschner, 1993 Properties of *Saccharomyces cerevisiae* wee1 and its differential regulation of p34CDC28 in response to G1 and G2 cyclins. *EMBO J.* 12: 3417–3426.
- De Bruin, R. A. M., W. H. McDonald, T. I. Kalashnikova, J. Yates, and C. Wittenberg, 2004 *Cln3* activates G1-specific transcription via phosphorylation of the SBF bound repressor *Whi5*. *Cell* 117: 887–898.
- Chan, R. K., and C. A. Otte, 1982 Physiological characterization of *Saccharomyces cerevisiae* mutants supersensitive to G1 arrest by a factor and alpha factor pheromones. *Mol. Cell. Biol.* 2: 21–29.
- Costanzo, M., J. L. Nishikawa, X. Tang, J. S. Millman, O. Schub *et al.*, 2004 CDK activity antagonizes *Whi5*, an inhibitor of G1/S transcription in yeast. *Cell* 117: 899–913.
- Cross, F., 1990 Cell cycle arrest caused by *CLN* gene deficiency in *Saccharomyces cerevisiae* resembles START-I arrest and is independent of the mating-pheromone signalling pathway. *Mol. Cell. Biol.* 10: 6482–6490.
- Cross, F. R., 1995 Starting the cell cycle: what's the point? *Curr. Opin. Cell Biol.* 7: 790–797.
- Cross, F. R., and K. Pecani, 2011 Efficient and rapid exact gene replacement without selection. *Yeast* 28: 167–179.
- Cross, F. R., and A. H. Tinkelenberg, 1991 A potential positive feedback loop controlling *CLN1* and *CLN2* gene expression at the start of the yeast cell cycle. *Cell* 65: 875–883.
- Cross, F. R., M. Yuste-Rojas, S. Gray, and M. D. Jacobson, 1999 Specialization and targeting of B-type cyclins. *Mol. Cell* 4: 11–19.
- Cross, F. R., V. Archambault, M. Miller, and M. Klovstad, 2002 Testing a mathematical model of the yeast cell cycle. *Mol. Biol. Cell* 13: 52–70.
- Dahmann, C., J. F. Diffley, and K. A. Nasmyth, 1995 S-phase-promoting cyclin-dependent kinases prevent re-replication by

- inhibiting the transition of replication origins to a pre-replicative state. *Curr. Biol.* 5: 1257–1269.
- Detweiler, C. S., and J. J. Li, 1998 Ectopic induction of Clb2 in early G1 phase is sufficient to block prereplicative complex formation in *Saccharomyces cerevisiae*. *Proc. Natl. Acad. Sci. USA* 95: 2384–2389.
- Dirick, L., and K. Nasmyth, 1991 Positive feedback in the activation of G1 cyclins in yeast. *Nature* 351: 754–757.
- Dirick, L., T. Böhm, and K. Nasmyth, 1995 Roles and regulation of Cln-Cdc28 kinases at the start of the cell cycle of *Saccharomyces cerevisiae*. *EMBO J.* 14: 4803–4813.
- Di Talia, S., J. M. Skotheim, J. M. Bean, E. D. Siggia, and F. R. Cross, 2007 The effects of molecular noise and size control on variability in the budding yeast cell cycle. *Nature* 448: 947–951.
- Donaldson, A. D., M. K. Raghuraman, K. L. Friedman, F. R. Cross, B. J. Brewer *et al.*, 1998 CLB5-dependent activation of late replication origins in *S. cerevisiae*. *Mol. Cell* 2: 173–182.
- Doncic, A., M. Falleur-Fettig, and J. M. Skotheim, 2011 Distinct interactions select and maintain a specific cell fate. *Mol. Cell* 43: 528–539.
- Drapkin, B. J., Y. Lu, A. L. Procko, B. L. Timney, and F. R. Cross, 2009 Analysis of the mitotic exit control system using locked levels of stable mitotic cyclin. *Mol. Syst. Biol.* 5: 328.
- Edelstein, A., N. Amodaj, K. Hoover, R. Vale, and N. Stuurman, 2010 Computer control of microscopes using manager. *Curr. Protoc. Mol. Biol.* Chapter 14: Unit14.20.
- Edelstein, A. D., M. A. Tsuchida, N. Amodaj, H. Pinkard, R. D. Vale *et al.*, 2014 Advanced methods of microscope control using μ Manager software. *J. Biol. Methods* 1: 1–10.
- Epstein, C. B., and F. R. Cross, 1992 CLB5: a novel B cyclin from budding yeast with a role in S phase. *Genes Dev.* 6: 1695–1706.
- Epstein, C. B., and F. R. Cross, 1994 Genes that can bypass the CLN requirement for *Saccharomyces cerevisiae* cell cycle START. *Mol. Cell. Biol.* 14: 2041–2047.
- Fitch, I., C. Dahmann, U. Surana, A. Amon, K. Nasmyth *et al.*, 1992 Characterization of four B-type cyclin genes of the budding yeast *Saccharomyces cerevisiae*. *Mol. Biol. Cell* 3: 805–818.
- Geng, Y., Q. Yu, E. Sicinska, M. Das, J. E. Schneider *et al.*, 2003 Cyclin E ablation in the mouse. *Cell* 114: 431–443.
- Ghiara, J. B., H. E. Richardson, K. Sugimoto, M. Henze, D. J. Lew *et al.*, 1991 A cyclin B homolog in *S. cerevisiae*: chronic activation of the Cdc28 protein kinase by cyclin prevents exit from mitosis. *Cell* 65: 163–174.
- Glotzer, M., A. W. Murray, and M. W. Kirschner, 1991 Cyclin is degraded by the ubiquitin pathway. *Nature* 349: 132–138.
- Hartwell, L. H., J. Culotti, J. R. Pringle, and B. J. Reid, 1974 Genetic control of the cell division cycle in yeast. *Science* 183: 46–51.
- Jaspersen, S. L., and D. O. Morgan, 2000 Cdc14 activates Cdc15 to promote mitotic exit in budding yeast. *Curr. Biol.* 10: 615–618.
- Jaspersen, S. L., J. F. Charles, R. L. Tinker-Kulberg, and D. O. Morgan, 1998 A late mitotic regulatory network controlling cyclin destruction in *Saccharomyces cerevisiae*. *Mol. Biol. Cell* 9: 2803–2817.
- King, R. W., R. J. Deshaies, J. M. Peters, and M. W. Kirschner, 1996 How proteolysis drives the cell cycle. *Science* 274: 1652–1659.
- Knapp, D., L. Bhoite, D. J. Stillman, and K. Nasmyth, 1996 The transcription factor Swi5 regulates expression of the cyclin kinase inhibitor p40SIC1. *Mol. Cell. Biol.* 16: 5701–5707.
- Koff, A., F. Cross, A. Fisher, J. Schumacher, K. Leguellec *et al.*, 1991 Human cyclin E, a new cyclin that interacts with two members of the CDC2 gene family. *Cell* 66: 1217–1228.
- Kõivomägi, M., E. Valk, R. Venta, A. Iofik, M. Lepiku *et al.*, 2011 Dynamics of Cdk1 substrate specificity during the cell cycle. *Mol. Cell* 42: 610–623.
- König, C., H. Maekawa, and E. Schiebel, 2010 Mutual regulation of cyclin-dependent kinase and the mitotic exit network. *J. Cell Biol.* 188: 351–368.
- Léopold, P., and P. H. O'Farrell, 1991 An evolutionarily conserved cyclin homolog from *Drosophila* rescues yeast deficient in G1 cyclins. *Cell* 66: 1207–1216.
- Levine, K., K. Huang, and F. R. Cross, 1996 *Saccharomyces cerevisiae* G1 cyclins differ in their intrinsic functional specificities. *Mol. Cell. Biol.* 16: 6794–6803.
- Levine, K., L. Kiang, M. D. Jacobson, R. P. Fisher, and F. R. Cross, 1999 Directed evolution to bypass cyclin requirements for the Cdc28p cyclin-dependent kinase. *Mol. Cell* 4: 353–363.
- Lew, D. J., and S. I. Reed, 1993 Morphogenesis in the yeast cell cycle: regulation by Cdc28 and cyclins. *J. Cell Biol.* 120: 1305–1320.
- Lew, D. J., V. Dulić, and S. I. Reed, 1991 Isolation of three novel human cyclins by rescue of G1 cyclin (Cln) function in yeast. *Cell* 66: 1197–1206.
- Loog, M., and D. O. Morgan, 2005 Cyclin specificity in the phosphorylation of cyclin-dependent kinase substrates. *Nature* 434: 104–108.
- Lu, Y., and F. R. Cross, 2010 Periodic cyclin-cdk activity entrains an autonomous cdc14 release oscillator. *Cell* 141: 268–279.
- Mendenhall, M. D., 1993 An inhibitor of p34CDC28 protein kinase activity from *Saccharomyces cerevisiae*. *Science* 259: 216–219.
- Murray, A. W., and M. W. Kirschner, 1989 Dominoes and clocks: the union of two views of the cell cycle. *Science* 246: 614–621.
- Murray, A. W., M. J. Solomon, and M. W. Kirschner, 1989 The role of cyclin synthesis and degradation in the control of maturation promoting factor activity. *Nature* 339: 280–286.
- Nasmyth, K., 1996 At the heart of the budding yeast cell cycle. *Trends Genet.* 12: 405–412.
- Oikonomou, C., and F. R. Cross, 2011 Rising cyclin-CDK levels order cell cycle events. *PLoS One* 6: e20788.
- Peter, M., and I. Herskowitz, 1994 Direct inhibition of the yeast cyclin-dependent kinase Cdc28-Cln by Far1. *Science* 265: 1228–1231.
- Pfleger, C. M., and M. W. Kirschner, 2000 The KEN box: an APC recognition signal distinct from the D box targeted by Cdh1. *Genes Dev.* 14: 655–665.
- Rahi, S. J., K. Pecani, A. Ondracka, C. Oikonomou, and F. R. Cross, 2016 The CDK-APC/C oscillator predominantly entrains periodic cell-cycle transcription. *Cell* 165: 475–487.
- Richardson, H. E., C. Wittenberg, F. Cross, and S. I. Reed, 1989 An essential G1 function for cyclin-like proteins in yeast. *Cell* 59: 1127–1133.
- Richardson, H., D. J. Lew, M. Henze, K. Sugimoto, and S. I. Reed, 1992 Cyclin-B homologs in *Saccharomyces cerevisiae* function in S phase and in G2. *Genes Dev.* 6: 2021–2034.
- Roberts, J. M., 1999 Evolving ideas about cyclins. *Cell* 98: 129–132.
- Schindelin, J., C. T. Rueden, M. C. Hiner, and K. W. Eliceiri, 2015 The ImageJ ecosystem: an open platform for biomedical image analysis. *Mol. Reprod. Dev.* 82: 518–529.
- Schmoller, K. M., J. J. Turner, M. Kõivomägi, and J. M. Skotheim, 2015 Dilution of the cell cycle inhibitor Whi5 controls budding-yeast cell size. *Nature* 526: 268–272.
- Schneider, C. A., W. S. Rasband, and K. W. Eliceiri, 2012 NIH image to ImageJ: 25 years of image analysis. *Nat. Methods* 9: 671–675.
- Schwob, E., and K. Nasmyth, 1993 CLB5 and CLB6, a new pair of B cyclins involved in DNA replication in *Saccharomyces cerevisiae*. *Genes Dev.* 7: 1160–1175.
- Schwob, E., T. Bohm, M. D. Mendenhall, and K. Nasmyth, 1994 The B-type cyclin kinase inhibitor p40SIC1 controls the

- G1 to S transition in *S. cerevisiae*. (erratum: Cell 84(1): following 174] Cell 79: 233–244.
- Sicinski, P., J. L. Donaher, S. B. Parker, T. Li, A. Fazeli *et al.*, 1995 Cyclin D1 provides a link between development and oncogenesis in the retina and breast. *Cell* 82: 621–630.
- Skotheim, J. M., S. Di Talia, E. D. Siggia, and F. R. Cross, 2008 Positive feedback of G1 cyclins ensures coherent cell cycle entry. *Nature* 454: 291–296.
- Toyn, J. H., A. L. Johnson, J. D. Donovan, W. M. Toone, and L. H. Johnston, 1997 The Swi5 transcription factor of *Saccharomyces cerevisiae* has a role in exit from mitosis through induction of the cdk-inhibitor Sic1 in telophase. *Genetics* 145: 85–96.
- Tyers, M., 1996 The cyclin-dependent kinase inhibitor p40SIC1 imposes the requirement for Cln G1 cyclin function at Start. *Proc. Natl. Acad. Sci. USA* 93: 7772–7776.
- Ubersax, J. A., E. L. Woodbury, P. N. Quang, M. Paraz, J. D. Blethrow *et al.*, 2003 Targets of the cyclin-dependent kinase Cdk1. *Nature* 425: 859–864.
- Wäsch, R., and F. R. Cross, 2002 APC-dependent proteolysis of the mitotic cyclin Clb2 is essential for mitotic exit. *Nature* 418: 556–562.
- Yeong, F. M., H. H. Lim, C. G. Padmashree, and U. Surana, 2000 Exit from mitosis in budding yeast: biphasic inactivation of the Cdc28-Clb2 mitotic kinase and the role of Cdc20. *Mol. Cell* 5: 501–511.
- Yuste-Rojas, M., and F. R. Cross, 2000 Mutations in CDC14 result in high sensitivity to cyclin gene dosage in *Saccharomyces cerevisiae*. *Mol. Gen. Genet.* 263: 60–72.

Communicating editor: S. Biggins